Atmos. Chem. Phys. Discuss., 11, 4599–4630, 2011
www.atmos-chem-phys-discuss.net/11/4599/2011/
doi:10.5194/acpd-11-4599-2011

Atmospheric Chemistry and Physics Discussions

Deriving the effect of wind speed on clean maritime aerosol optical properties using the A-Train satellites

V. P. Kiliyanpilakkil and N. Meskhidze

Department of Marine, Earth and Atmospheric Sciences, North Carolina State University, Raleigh, NC, USA

Received: 27 January 2011 – Accepted: 27 January 2011 – Published: 8 February 2011

Correspondence to: N. Meskhidze (nmeskhidze@ncsu.edu)

Published by Copernicus Publications on behalf of the European Geosciences Union.

Abstract

Relationship between "clean marine" aerosol optical properties and ocean surface wind speed is explored using remotely sensed data from the Cloud-Aerosol Lidar with Orthogonal Polarization (CALIOP) on board the CALIPSO satellite and the Advanced Microwave Scanning Radiometer (AMSR-E) on board the AQUA satellite. Detailed data analyses are carried out over 15 regions selected to be representative of different areas of the global ocean for the time period from June 2006 to June 2010. Based on remotely sensed optical properties the CALIPSO algorithm is capable of discriminating "clean marine" aerosols from other types often present over the ocean (such as urban/industrial pollution, desert dust and biomass burning). The global mean optical depth of "clean marine" aerosol at 532 nm (AOD_{532}) is found to be 0.052 ± 0.038. The mean layer integrated volume depolarization ratio of marine aerosols is 0.016 ± 0.012, the value representative of sea salt crystals. Integrated attenuated backscatter and color ratio of marine aerosols at 532 nm were obtained to be $0.003 \pm 0.002\,sr^{-1}$ and 0.530 ± 0.149, respectively. A logistic regression between AOD_{532} and 10-meter surface wind speed (U_{10}) revealed three distinct regions. For surface winds lower than $4\,m\,s^{-1}$, the mean CALIPSO-derived AOD_{532} is found to be 0.02 ± 0.003 with little dependency on the surface wind speed. For surface winds from $4\,m\,s^{-1}$ to $12\,m\,s^{-1}$, representing the dominant fraction of all available data, marine aerosol optical depth is linearly correlated with the U_{10}, with a slope of $0.0062\,s\,m^{-1}$. In this intermediate wind speed region, the AOD_{532} vs. U_{10} regression derived here is comparable to previously reported relationships. At very high wind speed values ($U_{10} > 18\,m\,s^{-1}$), the AOD_{532}-wind speed relationship showed a tendency toward leveling off, suggesting the existence of some maximum value for maritime AOD. Results of our calculations suggest that considerable improvements to both optical properties of marine aerosols and their production mechanisms can be achieved by discriminating "clean marine" aerosols (or sea salt particles) from all other types of aerosols present over the ocean.

ACPD
11, 4599–4630, 2011

1 Introduction

Marine aerosols play significant role in global energy budget; they influence the planetary radiation balance directly by scattering and absorbing sunlight, and indirectly by modifying cloud microphysical properties (Clarke and Kapustin, 2003; Murphy et al., 1998; Pierce and Adams, 2006). As cloud properties are most sensitive to the addition of particles when the background concentration is low (Platnick and Twomey, 1994), marine aerosols play crucial role in our understanding of the cloud-mediated effects of aerosols on climate.

Aerosols over the ocean are comprised of different natural and anthropogenic components such as sea salt, dust, urban/industrial pollution, biomass burning aerosols, biogenic particles, organic compounds, sulfates, and nitrates (Andreae, 2007). Although sea salt particles, frequently associated with "pure marine aerosol," are often a major component of aerosol mass over the remote oceanic regions (Prospero, 2002; Lewis and Schwartz, 2004), it was shown that sulfates from the oxidation of biogenic dimethylsulfide (DMS), and ocean produced organics could also contribute considerably to total aerosol budget (Shaw, 1983; Charlson et al., 1987; O'Dowd et al., 2004; Meskhidze and Nenes, 2006). Clean marine aerosols have been proposed to have two distinctly different sources which can be broadly classified as primary (associated with wind driven processes) and secondary (associated with gas-to-particle conversion). Starting with several contributions of Blanchard and Woodcock in the 1950s (Blanchard and Woodcock, 1957 and references therein), the bursting of rising air bubbles that have been injected below the sea surface by breaking waves, and the tearing of droplets from wave crests, have been understood to present the dominant production mechanisms of primary marine aerosol (Lewis and Schwartz, 2004; Schulz et al., 2004; Andreae and Rosenfeld, 2008). Measurements of freshly-emitted sea spray have revealed that bubble bursting processes, largely responsible for the production of sea salt aerosol, also controlled sea to air transfer of marine primary organic matter composed of biogenic secretions and bacterial/viral debris (O'Dowd et al., 2004;

ACPD
11, 4599–4630, 2011

Middlebrook et al., 1998; Leck and Bigg, 2005). Secondary aerosols of marine origin are derived from precursor biogenic volatile organic compounds (BVOCs) emitted by phytoplankton and macroalgae or by photolysis of chromophoric dissolved organic matter (CDOM) in the water column (Zhou and Mopper, 1997; O'Dowd and de Leeuw, 2007; Sellegri et al., 2008).

A number of studies devoted to investigating the effect of ocean emissions show that sea spray contribution to marine aerosol optical depth (AOD) can approach or even exceed values of 0.3, suggesting that under moderately high wind speed regimes marine emissions can rival that of anthropogenic plumes advecting out into marine environment (Mulcahy et al., 2008; O'Dowd et al., 2010). Previous modeling studies have suggested a wide range of estimates of the shortwave (SW) and net (shortwave and longwave) direct radiative effect, from -0.15 to $-2.2\,\mathrm{W\,m^{-2}}$ for the clear-sky and from -0.31 to $-1.1\,\mathrm{W\,m^{-2}}$ for the whole-sky global annual mean (Dobbie et al., 2003; Grini et al., 2002; Jacobson 2001; Takemura et al., 2002; Ayash et al., 2008; Ma et al., 2008). The estimates regarding sea salt's indirect radiative effect are even larger ranging from $-0.38\,\mathrm{W\,m^{-2}}$ to $-2.9\,\mathrm{W\,m^{-2}}$ (Ayash et al., 2008; Ma et al., 2008).

As correct representation of marine aerosol characteristics and their radiative effects are essential for accurate modeling of the climate system, the dependency of maritime aerosol optical properties on sea surface wind speed and sea state has been examined by numerous investigators. Based on the measurements from Minicoy Island in the Arabian Sea, Moorthy and Satheesh (2000) derived an exponential relationship between columnar AOD and surface wind speed. Smirnov et al. (2003a) studied the effects of surface wind speed on aerosol optical properties using ground based AErosol RObotic NETwork (AERONET) (Holben et al., 1998) located on Midway Island in the Pacific Ocean. Huang et al. (2010) derived relationship between AOD from Advanced Along-Track Scanning Radiometer (AATSR) onboard European Space Agency's Envisat and 10 m wind speed from the European Centre for Medium-Range Weather Forecasts (ECMWF). Glantz et al. (2009) reported a power-law fit between Sea-viewing Wide Field-of-view Sensor (SeaWiFS) retrieved AOD and ECMWF wind speed over

ACPD
11, 4599–4630, 2011

the Northern Pacific ocean. Based on the measurements of aerosol properties at the Mace Head atmospheric research station under moderately windy conditions, Mulcahy et al. (2008) established a power-law relationship between marine AOD and surface wind speed. Using a systematic comparison between multiple satellite retrieved surface wind speed values, MODIS-derived AOD, and aerosol fine mode fraction, Lehahn et al. (2010) managed to isolate the maritime component of AOD over the ocean and quantify its dependence on surface wind speed.

Although the effect of wind speed on marine aerosol optical properties was thoroughly studied over the last several decades, comprehensive quantification of marine aerosols using remotely-sensed and ground-based measurement data suffered from a number of difficulties. The sensors were not able to make explicit distinction of "clean marine" aerosols from ones influenced by the terrestrial sources (i.e., mineral dust, biomass burning, anthropogenic pollution). Passive instruments used in earlier studies of marine aerosol optical properties also could not give vertical distribution of aerosols over the ocean, could not retrieve aerosols over the regions with no sunlight (e.g., at night and north/south of the Arctic and the Antarctic Circles, respectively), above continuous cloud cover or beneath thin cirrus (Winker and Pelon, 2003).

In this study, we expand upon previous satellite remote sensing analyses by introducing a novel approach that allows an explicit distinction of "clean marine" aerosols properties from those of other aerosol subtypes through the use of the Cloud-Aerosol Lidar and Infrared Pathfinder Satellite Observation (CALIPSO) satellite. Due to its unique capabilities, such as accurate determination of the vertical location of aerosols, retrieval of aerosol properties during the night as well as the day, CALIPSO can give new insight into the marine aerosol wind relationship. Unlike passive imagers that typically have highest relative error at low optical depth values, uncertainty in CALIPSO optical depth retrieval is lowest at low AOD (Winker at al., 2009), making it suitable instrument for exploring optical properties of aerosols under clean marine conditions.

ACPD
11, 4599–4630, 2011

2 Data analysis and methods

The wind speed dependence of marine aerosol optical depth is estimated using four years (June 2006 to June 2010) of remotely sensed AOD data from the Cloud-Aerosol Lidar with Orthogonal Polarization (CALIOP) onboard the CALIPSO satellite and the surface wind speed data from the Advanced Microwave Scanning Radiometer for EOS (AMSR-E) onboard the AQUA satellite. Two different types of data analysis were carried out. In the general analysis, the physical and optical properties of the CALIOP marine aerosol layers were calculated over the entire global ocean, while in the detailed analysis, the datasets selected over numerous oceanic regions were compared to derive the relationship between maritime aerosol optical depth and surface wind speed.

2.1 Remotely sensed data/instruments

CALIPSO provides aerosol and cloud optical properties using a two wavelength (532 nm and 1064 nm) polarization sensitive lidar, CALIOP, an Imaging Infrared Radiometer (IIR), and a Wide Field Camera (WFC) (Winker et al., 2009; Hunt et al., 2009). The CALIPSO retrieval algorithm considers scattering properties from particles and molecules, where molecular scattering properties are determined from the Global Modeling and Assimilation Office (GMAO) meteorological data. The CALIPSO algorithm applies corrections to the aerosol optical properties and accounts for molecular scattering (Young and Vaughan, 2009; Vaughan et al., 2004., 2009; Omar et al., 2009; Liu et al., 2009). In this study we use Level 2, version 3.01 "clean marine" aerosol layer properties from CALIPSO, derived at 5 km horizontal resolution. The CALIPSO marine aerosol layer products were spatially and temporally collocated with Level 3, version 5 gridded AMSR-E-derived daily surface wind speed at $0.25^{\circ} \times 0.25^{\circ}$. As both sensors are located on satellites that are part of the A-Train constellation (CALIOP on the CALIPSO and AMSR-E on the Aqua) (Hu et al., 2008; Kittaka et al., 2011; L'Ecuyer and Jiang, 2010), virtually the same scene is viewed by the sensors as CALIPSO flies

ACPD
11, 4599–4630, 2011

about 75 s behind the Aqua satellite. Both CALIPSO lidar and AMSR-E are capable of collecting day and night observations (Hu et al., 2008). In this study AMSR-E wind speed and CALIPSO layer optical properties from both ascending (equatorial crossing time at 13:30 local time) and descending (equatorial crossing time at 01:30 local time) passes were used.

The CALIPSO algorithm is distinctive from other satellite algorithms in its capability to discriminate marine aerosols from other subtypes (such as clean continental, desert dust, polluted continental, polluted dust, and smoke) (Omar et al., 2009). The aerosol optical depth as well as extinction and backscatter profile retrievals require particulate extinction to backscatter ratio also known as lidar ratio (S_a). The S_a is an intensive aerosol property, i.e., a property that does not depend on a number density of the aerosol but rather on such physical and chemical properties as size distribution, shape and composition. The type and subtype information of the layer is used to estimate initial S_a, whereas a final S_a is derived by applying transmittance correction to the extinction processing (Omar et al., 2004, 2009; Young and Vaughan, 2009). Only the high confidence retrievals (aerosol layers with the same initial S_a and final S_a) are used in the current analysis (Kittaka et al., 2011). Level 2 version 3.01 CALIPSO aerosol subtypes are defined with 532-nm and 1064 nm lidar ratios as clean continental (35 ± 16 sr and 30 ± 17 sr), clean marine (20 ± 6 sr and 45 ± 23 sr), desert dust (40 ± 20 sr and 55 ± 17 sr), polluted continental (70 ± 25 sr and 30 ± 14 sr), polluted dust (55 ± 22 sr and 48 ± 24 sr), and biomass burning (70 ± 28 sr and 40 ± 24 sr) (Cattrall et al., 2005; Omar et al., 2005, 2009; Mielonen et al., 2009). In Level 2 aerosol layer products CALIPSO provides vertically resolved aerosol properties for up to 8 aerosol layers in a column and each layer is further classified into one of six aerosol subtypes. For most of the aerosol types size distributions and complex refractive indices of CALIPSO aerosol models are based on AERONET-derived model parameters. However, clean marine aerosol properties used in the CALIPSO aerosol-type identification algorithm are not derived from AERONET, as the marine aerosol cluster is comprised of a small number of records (<4% of the total) (Vaughan et al., 2004). Therefore, the CALIPSO

ACPD
11, 4599–4630, 2011

marine aerosol model is derived from the size distribution parameters measured during the Shoreline Environmental Aerosol Study (SEAS) experiment (Masonis et al., 2003; Omar et al., 2004, 2009). In such model clean marine aerosols are expected to behave like a sea salt. However, measurements often report S_a values different from sea salt (Welton et al., 2002; Omar et al., 2009), suggesting that in certain regions sea spray optical properties can be considerably different from sea salt. Because of this, our data analysis is expected to be mainly representative of sea salt particles and not the other forms of natural marine aerosols (i.e., DMS-oxidized sulfate particles and marine primary and secondary organics).

The CALIOP separates clouds and aerosols and provides the cloud-aerosol discrimination (CAD) score for each layer (Liu et al., 2004, 2005, 2009; Vaughan et al., 2005). The standard CAD scores in the CALIPSO layer products range from −100 to 0 for aerosols and from 0 to +100 for clouds. Larger absolute value of CAD indicates higher confidence in the aerosol-cloud feature classification. The CALIPSO aerosol optical depths are provided at wavelengths 532 nm and 1064 nm. To extract marine aerosol types and the corresponding aerosol optical thicknesses, we have used CAD score of −70 to −100 and condition of initial S_a equal to final S_a which gives high confidence cloud cleared optical thickness layer data (Kittaka et al., 2011; Liu et al., 2009; Omar et al., 2009). To reduce uncertainties and increase quality assessment and reliability of layer optical depth, only aerosol layers corresponding to values from 0 to 0.01 sr^{-1} of integrated attenuated backscatter at 532 nm, values from 0 to 0.1 of estimated uncertainty of layer optical depth at 532 nm, and values from 0 to 2.0 of integrated attenuated total color ratio are used in the current analysis. The information provided by the layer integrated volume depolarization ratio, extinction quality control values, and opacity flag of the layers are also used to retrieve high confidence aerosol layers (Kittaka et al., 2011; Liu et al., 2005; http://eosweb.larc.nasa.gov/PRODOCS/calipso/Quality_Summaries/CALIOP_L2LayerProducts_3.01.html).

As part of NASA's Aqua satellite's global hydrology mission, over the oceans AMSR-E derives wind speed, sea surface temperature, atmospheric water vapor, cloud

ACPD
11, 4599–4630, 2011

water, and rain rate (Wentz and Meissner, 2000, 2007; Wentz et al., 2003). Passive microwave frequencies used by AMSR-E sensor allow it to "see" through clouds, thus providing continuous global surface wind observations (Wentz et al., 2003). The value of AMSR-E-derived 10 m daily surface wind speed (U_{10}) over the sea surface is determined by the surface roughness (caused by the wind stress) and is processed based on National Centers for Environmental Prediction (NCEP) reanalysis wind direction. Missing data can be caused by regions of sun glint, near sea ice, and proximity to land (~50 km) (Wentz and Meissner, 2007). The AMSR-E wind speed was validated with surface buoy and other satellite measured wind speeds (Konda et al., 2009; Kutsuwada et al., 2009; Wentz et al., 2003).

2.2 Data selection and analysis

The regression statistics for the dependency of maritime aerosol optical properties on U_{10} were calculated for the selected 15 regions of interest covering all the major parts of the global oceans (see Fig. 1a and Supplement Table S1). Although CALIPSO can distinguish different aerosol species, to minimize the contribution from terrestrial sources the regions were selected to be away from the known transport pathways of anthropogenic pollutants and mineral dust. The midpoint of each 5 km high confidence single-layer aerosol data were spatially and temporally collocated with the gridded ($0.25^\circ \times 0.25^\circ$) AMSR-E-derived U_{10}. Previous studies have shown that due to the downward propagations of bias errors into detected layers, the incorrect choice of S_a for the upper aerosol layers may cause errors in transmission corrections, causing large uncertainties for multi-layer aerosol retrievals (Winker et al., 2009; Weitkamp, 2005; Young and Vaughan, 2009). Data analyses carried out in this study revealed (see below) that the vast majority of marine aerosol layers (both layer bases and layer tops) were placed within 2 km of the mean sea level. Therefore, to reduce the erroneous classification of elevated aerosol layers over the ocean (Omar et al., 2009), only single-layer clean marine AODs below 2 km height above sea level were used for the

ACPD
11, 4599–4630, 2011

analysis. Collocated aerosol measurements for the selected regions were merged together and the resultant dataset was sorted into bins based on the wind speed. The bins were spaced in 1 m s^{-1} increments between $0 < U_{10} \leq 29$ m s^{-1}.

3 Results and discussion

3.1 Physical and optical properties of the CALIOP marine aerosol layers

The available CALIPSO data products can be analyzed in terms of aerosol extensive and intensive properties. Extensive parameters depend directly on particulate amount within the scattering volume, while intensive properties are independent of aerosol loading and depend only on optical properties as determined by aerosol composition, size and shape (Vaughan et al., 2004; Rogers et al., 2009). Figure 1 shows global seasonal maps of CALIPSO-derived maritime aerosol extensive property – optical depth. This figure demonstrates large spatial and temporal variations in maritime AOD at 532 nm (AOD_{532}). CALIPSO-derived maritime AOD at 1064 nm (AOD_{1064}) is also shown in Supplement (Fig. S1), although not included in the current analysis due to potential calibration problems (D. M. Winker, personal communication, 2010). Inspection of Fig. 1 shows that the largest values of AOD_{532} occur over the regions with elevated surface wind speed (i.e., northern and southern oceans), with the highest values found over the Southern Hemisphere mid-latitude oceans during austral winter (JJA) season. Regions of moderate winds typically show relatively low values of AODs. The exceptions are the regions downwind from dust and/or pollution sources such as mid-latitude North Atlantic Ocean and the Bay of Bengal (BoB), suggesting that some dust/pollution aerosols might have been misclassified as sea salt (see Fig. 1). Figure 1c shows sporadic retrievals of aerosols over BoB during the summer season, most likely due to thick, extensive cloud cover associated with the intense summertime monsoon season. The global mean AOD_{532} for single-layer marine aerosol is found to be 0.052 ± 0.038. The calculated AOD_{532} is consistent with the baseline

ACPD
11, 4599–4630, 2011

aerosol over the Pacific ($AOD_{500} = 0.052$) and Atlantic ($AOD_{500} = 0.071$) Oceans, reported by Kaufman et al. (2001). Calculated global mean AOD_{532} is also in a good agreement with $AOD_{500} = 0.06$, the most frequently occurring value of aerosol optical depth over the Central Pacific Ocean (Smirnov et al., 2003a, b) and within the range $0.02 < AOD_{550} < 0.067$ of sixteen global models participated in the Aerosol Comparisons between Observations and Models (AeroCom) Experiment-A (Rind et al., 2009). The frequency distribution of CALIPSO lidar marine aerosol layer AOD_{532} for 15 selected regions over the time period of June 2006 to June 2010 is shown in Fig. 2. It was found that approximately 99.5% of clean marine aerosol layers had $AOD_{532} < 0.2$, with $AOD_{532} = 0.03$ being the most frequently occurring value.

The vertical distribution of maritime aerosols was obtained by detailed inspection of the frequency of occurrences of marine aerosols with different layer top and layer base altitudes. Figure 3 shows that marine aerosols are generally confined within 2 km above mean sea level. For the entire study period, virtually all marine aerosol layer bases were placed below 0.5 km and 96% of aerosol layer tops were found to be below 2 km above sea level (Fig. 3), suggesting that the 2 km layer threshold selected in this study captures the majority of maritime aerosols. This result is in a good agreement with Kaufman et al. (2005) who, based on correlation between the wind speed and the AOD, suggested that sea salt aerosols should reside largely in the lowest 500 m of the atmosphere.

Intensive scattering properties of aerosols, such as color ratio (the ratio of aerosol backscatter at the two wavelengths) and aerosol depolarization ratio are also examined to gain some more insight into maritime aerosol optical properties. Particle sizes for most maritime aerosols exhibit a spectrally dependent scattering efficiency. Due to diffraction of light, large particles are expected show more forward scattering (extinction) (Weitkamp, 2005; Hu et al., 2007). Figure 4a shows that for the majority of layer-integrated aerosols examined over the selected fifteen regions, β_{532} is greater than β_{1064}, indicating the dominance of coarse mode sea salt aerosols. The larger values of β_{532} compared to β_{1064} (smaller backscatter at 1064 nm than that at 532) resulting

ACPD
11, 4599–4630, 2011

in values of layer-integrated attenuated total color ratio ($\chi = \beta_{1064}/\beta_{532}$) from ~0.4 to 0.7 (Fig. 4b), consistent with the expected values for the maritime aerosols (Vaughan et al., 2004; Liu et al., 2005; Hess et al., 1998). The integrated attenuated backscatter of single-layer marine aerosols averaged over the entire study period over the selected 15 regions were found to be $\beta_{532} = 0.003 \pm 0.002\,\mathrm{sr}^{-1}$ and $\beta_{1064} = 0.002 \pm 0.001\,\mathrm{sr}^{-1}$, yielding $\chi = 0.530 \pm 0.149$.

Another intensive property of aerosols, depolarization ratio (or particle non-sphericity) can provide an indication of aerosol shape. Deliquesced sea salt particles are expected to exhibit low depolarization (when neglecting multiple scattering), whereas irregularly shaped particles (e.g., dust) could significantly depolarize the backscattered signal (Liu et al., 2005; Gobbi et al., 2000; Murayama et al., 2001). The volume depolarization ratio, i.e., the ratio of the perpendicular and parallel components of the total backscatter ($\delta_v = \frac{\beta_\perp}{\beta_\parallel}$), is directly related to the hydration state of the sea salt. Figure 4c shows that the majority of maritime aerosols had layer-integrated volume depolarization ratios at 532 nm from 0.005 to 0.05, consistent with linear depolarization ratios reported for sea salt crystals (0.08 ± 0.01) and deliquesced droplets (0.01 ± 0.001) (Sakai et al., 2010). The four year mean layer-integrated volume depolarization ratio of single-layer marine aerosols examined in this study $\delta_v = 0.016 \pm 0.012$.

Overall, detailed analyses of clean marine aerosols intensive scattering properties suggest that large majority of the CALIPSO retrievals in selected fifteen regions had physical and optical properties characteristic of sea salt. In the next chapter CALIPSO retrievals will be used to derive relationship between surface wind speed and maritime aerosol optical depth. Potential differences between CALIPSO-retrieved "clean marine" aerosols and natural maritime aerosols will also be discussed.

ACPD
11, 4599–4630, 2011

3.2 Regression statistics for AOD_{532} – wind speed relationships

The relationship between collocated CALIPSO-AOD_{532} and AMSR-E wind speed at selected marine regions is shown on Fig. 5. According to Fig. 5 the majority of all the AOD_{532}retrievals (84.4% of all available data) fall between $2\,m\,s^{-1} < U_{10} \leq 12 ms^{-1}$ wind speed values. Our calculations indicate that the remaining number of retrievals fall between $12 < U_{10} \leq 24\,ms^{-1}$ wind speed values (14% of retrievals or 62 037 instances) and $U_{10} \leq 2\,m\,s^{-1}$ (1.6% of retrievals or 6880 instances). Although very few data points are available for the wind speeds above $24\,m\,s^{-1}$ (0.02% of retrievals or 89 instances) these data point were also included in the current study for the completeness. Removal of these points also does not change the conclusions drawn from the data analysis. Using the MATLAB curve fitting tool we have developed a logistic function for the CALIPSO-derived AOD_{532} and AMSR-E wind speed relationship. The results of our analysis show that the logistic regression

$$AOD_{532} = \frac{-1.5}{11.9+1.102 \cdot e^{0.215 \cdot U_{10}}} + 0.1353$$

provides the best fit ($R^2 = 0.97$) for maritime aerosol optical depth and 10-meter surface wind speed relationship. Figure 5 shows that there are three distinct regions in AOD versus U_{10} curve. For the $U_{10} \leq 4\,m\,s^{-1}$ maritime aerosol optical depth is only weakly related to wind speed. For the intermediate wind speed values $4 < U_{10} \leq 12\,m\,s^{-1}$, AOD_{532} increases qasi-linearly with the increase in surface wind. Finally, for higher wind speed values ($U_{10} > 18\,m\,s^{-1}$) the aerosol effects on optical turbidity of air appear to level off.

On Fig. 6 the logistic relationship for CALIPSO-AOD_{532} and AMSR-E wind speed is compared to those derived from previous studies. Parameters for the current and other regression statistics are summarized in Table 1. Figure 6 shows that the relationship derived here is generally comparable to previously published data; however some considerable differences are worth pointing out.

ACPD
11, 4599–4630, 2011

For $U_{10} \leq 4\,\mathrm{m\,s^{-1}}$, the mean CALIPSO derived AOD_{532} of marine aerosols is found to be roughly 0.02 ± 0.003. Figure 6 shows that at low wind speed values CALIPSO-derived AOD is comparable to $\mathrm{AOD}_{550,\mathrm{cm}}$ the coarse mode aerosol component of the wind induced maritime aerosol optical depth derived by Lehahn et al. (2010). However, Fig. 6 also shows that CALIPSO-AOD_{532} is roughly a factor of 3 lower than $\mathrm{AOD}_{550,\mathrm{m}}$, the total (sum of coarse and fine mode) maritime aerosol optical depth calculated using Lehahn et al. (2010) relationship. Our estimated AOD_{532} is also considerably lower than one calculated using the liner relationship of Smirnov et al. (2003a) ($\mathrm{AOD}_{500,\mathrm{SM}}$) and AOD derived by Huang et al. (2010) ($\mathrm{AOD}_{550,\mathrm{H}}$), but comparable to values derived from Glantz et al. (2009) regression relationship ($\mathrm{AOD}_{555,\mathrm{GL}}$). It is interesting to note that the physical mechanism for the weak dependence of maritime aerosol optical depth on surface wind speed at low wind values was suggested to be associated with a threshold wind speed of $\sim 4\,\mathrm{m\,s^{-1}}$, above which ocean surface waves start breaking, initiating the white cap formation and bursting of the entrained bubbles (Glantz et al., 2009 and references therein). However, the large discrepancy between CALIPSO-retrieved AOD_{532} values and the ones reported in other studies also points to the likelihood that background maritime AOD under low wind conditions may have considerable non-sea salt (i.e., DMS-oxidized sulfate particles and marine organics) component. However, potential misclassification of terrestrial fine mode aerosols (e.g., pollution, smoke and dust) in previous works also cannot be discarded.

For an intermediate wind speed values $4 < U_{10} \leq 12\,\mathrm{m\,s^{-1}}$ the dominant production mechanism for sea salt aerosols is the bursting of rising air bubbles. Figure 6 shows that there is a similar qasi-liner (or linear) dependence of AOD on surface wind speed in all parameterizations. According to this figure the main difference between our logistic relationship and the linear regression of Smirnov et al. (2003a) and Huang et al. (2010) is the low-wind component of AOD.

Figure 6 also shows that above wind speed values $\sim 12\,\mathrm{m\,s^{-1}}$ current CALIPSO-derived AOD_{532} values are lower compared to other regressions. Figure 6 shows the discrepancies are particularly pronounced between the AOD values derived in this

ACPD
11, 4599–4630, 2011

study and the power law relations of Mulcahy et al. (2008) and Glantz et al. (2009). At high wind speeds, the power law relations show AOD values well above 0.3. It was shown that for the wind speed values below 15 m s^{-1}, the relationship of Mulcahy et al. (2008) compares well to open-ocean MODIS-derived AODs, while at wind speeds above 15 m s^{-1}, Mulcahy et al. (2008) parameterization predicts higher values compared to satellite retrievals (O'Dowd et al., 2010). Overall, it is difficult to compare AOD values predicted by our logistic relationship with previously published regression statistics, as the past data analyses are typically limited to surface wind speed values below 20 m s^{-1}.

According to Fig. 6 CALIPSO-derived AOD_{532} tends to level off (and even decrease) at very high wind speeds, suggesting the existence of some perhaps a maximum value for maritime AOD. Although data sets for aerosol loadings under very high wind speed values obtained in different studies often show conflicting results (e.g., Pant et al., 2008), number of investigators do report a decrease in sea salt aerosol production with the increase in surface wind speed. Exton et al. (1985) reported that above 13 m s^{-1}, the measured amount of airborne material in maritime airmasses remained constant or decreased slightly with increasing wind speed. Barteneva et al. (1991) also noticed no increase in the particle concentrations with wind speeds over 15 m s^{-1}. During a severe cyclonic storm over south Indian Ocean Pant et al. (2008) also reported reduction in total aerosol number concentration with increase in the wind speed from 16 to 22 m s^{-1} after which aerosol number remained at nearly constant value up to the maximum wind speed of 33 m s^{-1}. The reason for such resistance of volumetric loading of aerosols to increase in wind speed values was explained by the presence of very large sea salt particles. At wind speeds in excess of ~12 m s^{-1} mechanism for sea spray generation is via mechanical disruption of wave crests (Exton et al., 1985; Wang and Street, 1978; Monahan, 1986; Lewis and Schwartz, 2004). The spume drops torn from the wave crests have relatively large sizes starting from 20 µm and reaching more than 500 µm (Andreas, 2002). Such large spume drops disperse and re-deposit more efficiently on the sea surface and may lead to collection of small aerosols during

ACPD
11, 4599–4630, 2011

their descend (Exton et al., 1985; Pant et al., 2008). However, it is also plausible that leveling off CALIPSO-AOD_{532} seen at very high wind speed values is a retrieval artifact. At stronger wind speeds there are increased chances that the CALIPSO lidar signal is contaminated with multiple scattering effects from whitecaps, correction for which is not included in current CALIPSO aerosol algorithm. Hu et al. (2008) noticed significant improvements in relationship between AMSR-E wind speed and CALIPSO lidar backscatter when they applied whitecaps correction in their analysis for higher wind speeds. Further study is required to evaluate the maritime aerosol AOD behavior under very high wind conditions.

4 Summary and conclusion

Analysis of remotely sensed data for maritime aerosol optical depth and surface wind speed values has been conducted over the global ocean covering wide range of wind speed and AOD conditions. To exclude the contribution from non-marine aerosol such as urban/industrial pollution, desert dust and biomass burning the maritime aerosol AOD_{532} was calculated using CALIPSO derived "clean marine" aerosol subtype. Daily surface wind speed data were obtained from the AMSR-E. Detailed data analyses were carried out over 15 regions selected to be representative of different areas of the global oceans for the time period from June 2006 to June 2010. Conceptual relationship between CALIPSO-retrieved AOD_{532} and AMSR-E wind speed was derived using a total of over 443 000 collocated data points. The global mean single-layer AOD_{532} was found to be 0.052 ± 0.038, consistent with the previous estimates of baseline aerosol optical depth over the Pacific and Atlantic Oceans. The mean layer integrated volume depolarization ratio of marine aerosols was found to be 0.016 ± 0.012, representative of sea salt crystals. Integrated attenuated backscatter and the color ratio of the marine aerosols at 532 nm were found to be $0.003 \pm 0.002\ sr^{-1}$ and 0.530 ± 0.149, respectively.

ACPD
11, 4599–4630, 2011

Derived logistic regression between CALIPSO-retrieved AOD_{532} and AMSR-E wind speed indicates weak relationship at low wind speed values ($U_{10} \leq 4\,m\,s^{-1}$). This result is consistent with previous studies, suggesting that AOD_{532} at surface wind speed $\leq 4\,m\,s^{-1}$ can be viewed to be representative of background maritime aerosol with little dependence on surface wind speed. Our data analysis shows that under such low wind conditions CALIPSO-derived AOD_{532} is roughly a factor of 2 lower compared to previously reported values of total maritime aerosol AOD, but consistent with its wind induced component (Lehahn et al., 2010). We proposed that such inconsistency is likely to be caused by potential underestimation of marine biogenic sources of aerosol by CALIPSO and/or misclassification of terrestrial fine mode aerosols (e.g., pollution, smoke and dust) in previous works. Studies show that ocean derived sulfate and organics can contribute considerably to total aerosol budget, particularly under low wind conditions when bursting of the entrained air bubbles is rather ineffective mechanism for production of sea salt. We suggest that the constant lidar ratio of 20 sr (at 532 nm) used for high confidence marine aerosols in current analysis may not be characteristic for all types of natural maritime aerosols and could lead to potential underestimation of biogenic fraction of ocean derived aerosols. The lidar ratios as high as 33 ± 6 sr (at 523 nm) have been reported in the absence of any continental influence (Welton et al., 2002).

At an intermediate wind speed values ($4 < U_{10} \leq 12\,m\,s^{-1}$), the logistic regression relationship derived in this study between clean marine aerosol and surface wind speed has a constant slope of $0.0062\,s\,m^{-1}$. Our calculations suggest that in this intermediate range, representing the dominant fraction of all available data, CALIPSO-derived AOD_{532} dependence on U_{10} is consistent with previously reported regression relationships.

At high wind speed values ($U_{10} > 12\,m\,s^{-1}$) our logistic regression predicts AOD_{532} values lower than ones derived using power-law and linear relationships. Analysis of CALIPSO-retrieved AOD_{532} and AMSR-E wind speed values suggests that for sea spray generation via mechanical disruption of wave crests aerosol effects on optical

ACPD
11, 4599–4630, 2011

turbidity of atmosphere appear to level off at the highest wind speed values, indicating the existence of some finite maritime AOD values. However, such conclusions may also be influenced by potential contamination of CALIPSO lidar signal by whitecaps and further study is required to better evaluate the maritime aerosol AOD behavior under very high wind conditions.

Supplementary material related to this article is available online at: http://www.atmos-chem-phys-discuss.net/11/4599/2011/acpd-11-4599-2011-supplement.pdf.

Acknowledgements. This research was supported by the Office of Science (BER), US Department of Energy, grant no. DE-FG02-08ER64508 and by the National Science Foundation through the grant no ATM-0826117. We thank Yongxiang Hu, Alexander Smirnov and Santiago Gassó for fruitful discussions. The authors gratefully acknowledge the CALIPSO and AMSR-E Teams for their effort in making the data available. CALIPSO data were obtained from the NASA Langley Research Center Atmospheric Science Data Center. AMSR-E data are produced by Remote Sensing Systems and sponsored by the NASA Earth Science MEaSUREs DISCOVER Project and the AMSR-E Science Team. Data are available at www.remss.com.

References

Andreae, M. O.: Aerosols before pollution, Science, 315, 5808, 50–51, doi:10.1126/science.1136529, 2007.

Andreae, M. O. and Rosenfeld, D.: Aerosol-cloud-precipitation interactions. Part 1, The nature and sources of cloud-active aerosols, Earth-Sci. Rev., 89, 13–41, doi:10.1016/j.earscirev.2008.03.001, 2008.

Andreas, E. L.: A review of the sea spray generation function for the open ocean,Atmosphere-Ocean Interactions, W. A. Perrie, Ed., WIT Press, Southampton, UK, Vol. 11–46, 2002.

Ayash, T., Gong, S., and Jia, C. Q.: Direct and indirect shortwave radiative effects of sea salt aerosols, J. Clim., 21, 3207–3220, doi:10.1175/2007JCLI2063.1, 2008.

ACPD
11, 4599–4630, 2011

Barteneva, O. D., Nikitinskaya, N. I., Sakunov, G. G., and Veselova, L. K.: Atmospheric transmittance in the visible and near IR spectral range, 224 pp., Gidrometeoizdat, Leningrad, 1991 (in Russian).
Blanchard, D. C. and Woodcock, A. H.: Bubble formation and modification in the sea and its meteorological significance, Tellus, 9, 145–158, 1957.
Cattrall, C., Reagan, J., Thome, K., and Dubovik, O.: Variability of aerosol and spectral lidar and backscatter and extinction ratios of key aerosol types derived from selected Aerosol Robotic Network locations, J. Geophys. Res., 110, D10S11, doi:10.1029/2004JD005124, 2005.
Charlson, R. J., Lovelock, J. E., Andreae, M. O., and Warren, S. G.: Oceanic phytoplankton, atmospheric sulphur, cloud albedo and climate, Nature, 326, 6114, 655–661, doi:10.1038/326655a0, 1987.
Clarke, A. D. and Kapustin, V. N.: The Shoreline Environment Aerosol Study (SEAS): A context for marine aerosol measurements influenced by a coastal environment and long-range transport, J. Atmos. Oceanic Technol., 20, 1351–1361, 2003.
Dobbie, S., Li, J., Harvey, R., and Chylek, P.: Sea salt optical properties and GCM forcing at solar wavelengths, Atmos. Res., 65, 211–233, 2003.
Exton, H. J., Latham, J., Park, P. M., Perry, S. J., Smith, M. H., and Allan R. R.: The production and dispersal of marine aerosol, Q. J. R. Meteorol. Soc., 111, 817–837, 1985.
Ghan, S., Laulainen, N., Easter, R., Wagener, R., Nemesure, S., Chapman, E., Zhang, Y., and Leung, R.: Evaluation of aerosol direct radiative forcing in MIRAGE, J. Geophys. Res., 106, 5295–5316, doi:10.1029/2000JD900502, 2001.
Glantz, P., Nilsson, E., and von Hoyningen-Huene, W.: Estimating a relationship between aerosol optical thickness and surface wind speed over the ocean, Atmos. Res., 92, 58–68, doi:10.1016/j.atmosres.2008.08.010, 2009.
Gobbi, G. P., Barnaba, F., Giorgi, R., and Santacasa, A.: Altitude resolved properties of a Saharan dust event over the Mediterranean, Atmos. Environ., 34, 5119– 5127, doi:10.1016/S1352-2310(00)00194-1, 2000.
Grini, A., Myhre, G., Sundet, J. K., and Isaksen, I. S. A.: Modeling the annual cycle of sea salt in the global 3-D model Oslo CTM2: Concentrations, fluxes, and radiative impact, J. Clim., 15, 1717–1730, 2002.
Hess, M., Koepke, P., and Schult, I.: Optical properties of aerosols and clouds: The software package OPAC, B. Am. Meteor. Soc., 79, 831–844, 1998.
Holben, B. N., Eck, T. F., Slutsker, I., Tanre, D., Buis, J. P., Setzer, A., Vermote, E., Reagan, J.

ACPD
11, 4599–4630, 2011

A., Kaufman, Y. J., Nakajima, T., Lavenu, F., Jankowiak, I., and Smirnov, A.: AERONET – A federated instrument network and data archive for aerosol characterization, Remote Sens. Environ., 66, 1–16, 1998.

Hoose, C., Kristjánsson, J. E., Iversen, T., Kirkevåg, A., Seland, Ø., and Gettelman, A.: Constraining cloud droplet number concentration in GCMs suppresses the aerosol indirect effect, Geophys. Res. Lett., 36, L12807, doi:10.1029/2009GL038568, 2009.

Hunt, W., Winker, D., Vaughan, M., Powell, K., Lucker, P., and Weimer, C.: CALIPSO lidar description and performance assessment, J. Atmos. Ocean. Tech., 26, 1214–1228, 2009.

Hu, Y., Vaughan, M., McClain, C., Behrenfeld, M., Maring, H., Anderson, D., Sun-Mack, S., Flittner, D., Huang, J., Wielicki, B., Minnis, P., Weimer, C., Trepte, C., and Kuehn, R.: Global statistics of liquid water content and effective number concentration of water clouds over ocean derived from combined CALIPSO and MODIS measurements, Atmos. Chem. Phys., 7, 3353–3359, doi:10.5194/acp-7-3353-2007, 2007.

Hu, Y., Stamnes, K., Vaughan, M., Pelon, J., Weimer, C., Wu, D., Cisewski, M., Sun, W., Yang, P., Lin, B., Omar, A., Flittner, D., Hostetler, C., Trepte, C., Winker, D., Gibson, G., and Santa-Maria, M.: Sea surface wind speed estimation from space-based lidar measurements, Atmos. Chem. Phys., 8, 3593–3601, doi:10.5194/acp-8-3593-2008, 2008.

Huang, H., Thomas, G. E., and Grainger, R. G.: Relationship between wind speed and aerosol optical depth over remote ocean, Atmos. Chem. Phys., 10, 5943–5950, doi:10.5194/acp-10-5943-2010, 2010.

Jacobson, M. Z.: Global direct radiative forcing due to multicomponent anthropogenic and natural aerosols, J. Geophys. Res., 106, 1551–1568, doi:10.1029/2000JD900514, 2001.

Kaufman, Y., Smirnov, A., Holben, B., and Dubovik, O.: Baseline maritime aerosol: methodology to derive the optical thickness and scattering properties, Geophys. Res. Lett., 17, 3251–3254, doi:10.1029/2001GL013312, 2001.

Kaufman, Y. J., Koren, I., Remer, L. A., Tanré, D., Ginoux, P., and Fan, S.: Dust transport and deposition observed from the Terra-Moderate Resolution Imaging Spectroradiometer (MODIS) spacecraft over the Atlantic Ocean, J. Geophys. Res., 110, D10S12, doi:10.1029/2003JD004436, 2005.

Kittaka, C., Winker, D. M., Vaughan, M. A., Omar, A., and Remer, L. A.: Intercomparison of column aerosol optical depths from CALIPSO and MODIS-Aqua, Atmos. Meas. Tech., 4, 131–141, doi:10.5194/amt-4-131-2011, 2011.

Konda, M., Ichikawa, H., and Tomita, H.: Wind speed and latent heat flux retrieved by simul-

ACPD
11, 4599–4630, 2011

taneous observation of multiple geophysical parameters by AMSR-E, J. Remote Sens. Soc. Jpn, 29(1), 191–198, 2009.
Kutsuwada, K., Koyama, M., and Morimoto, N.: Validation of gridded surface wind products using spaceborne microwave sensors and their application to air-sea interaction in the Kuroshio Extension region, J. Remote Sens. Soc. Jpn, 29(1), 179–190, 2009.
Leck, C. and Bigg, E. K.: Source and evolution of the marine aerosol - A new perspective, Geophys. Res. Lett., 32, L19803, doi:10.1029/2005GL023651, 2005.
Lehahn, Y., Koren, I., Boss, E., Ben-Ami, Y., and Altaratz, O.: Estimating the maritime component of aerosol optical depth and its dependency on surface wind speed using satellite data, Atmos. Chem. Phys., 10, 6711–6720, doi:10.5194/acp-10-6711-2010, 2010.
L'Ecuyer, T. S. and Jiang, J. H.: Touring the atmosphere aboard the A-Train, Phys. Today, 63(7), 36–41, doi:10.1063/1.3463626, 2010.
Lewis, R. and Schwartz, S. E.: Sea Salt Aerosol Production: Mechanisms, Methods, Measurements, and Models – A Critical Review, Geophysical monograph 152, American Geophysical Union, Washington, DC, 413 pp., 2004.
Liu, Z., Omar, A. H., Hu, Y., Vaughan, M. A., and Winker, D. M.: CALIOP Algorithm Theoretical Basis Document, Part 3: Scene Classification Algorithms, Release 1.0, PC-SCI-202, NASA Langley Research Center, Hampton, VA, 56, available at: http://www-calipso.larc.nasa.gov/resources/pdfs/PC-SCI-202_Part3_v1.0.pdf, 2005.
Liu, Z., Vaughan, M. A., Winker, D. M., Hostetler, C. A., Poole, L., Hlavka, D., Hart, W., and McGill, M.: Use of probability distribution functions for discriminating between cloud and aerosol in lidar backscatter data, J. Geophys. Res., 109, D15202, doi:10.1029/2004JD004732, 2004.
Liu, Z., Vaughan, M. A., Winker, D. M., Kittaka, C., Getzewich, B. J., Kuehn, R. E., Omar, A. H., Powell, K., Trepte, C. R., and Hostetler, C. A.: The CALIPSO Lidar Cloud and Aerosol Discrimination: Version 2 Algorithm and Initial Assessment of Performance, J. Atmos. Ocean. Tech., 26, 1198–1213, doi:10.1175/2009JTECHA1229.1, 2009.
Lohmann, U., Feichter, J., Penner, J., and Leaitch, R.: Indirect effect of sulfate and carbonaceous aerosols: A mechanistic treatment, J. Geophys. Res., 105(D10), 12193–12206, doi:10.1029/1999JD901199, 2000.
Ma, X., von Salzen, K., and Li, J.: Modelling sea salt aerosol and its direct and indirect effects on climate, Atmos. Chem. Phys., 8, 1311–1327, doi:10.5194/acp-8-1311-2008, 2008.
Masonis, S. J., Anderson, T. L., Covert, D. S., Kapustin, V., Clarke, A. D., Howell, S., and Moore,

ACPD
11, 4599–4630, 2011

K.: A study of the extinction- to-backscatter ratio of marine aerosol during the Shoreline Environment Aerosol Study, J. Atmos. Ocean. Tech., 20, 1388–1402, 2003.
Meskhidze, N. and Nenes A.: Effects of ocean ecosystem on marine aerosol-cloud interaction, Adv. in Meteorol., 2010, 239808, doi:10.1155/2010/239808, 2010.
Middlebrook, A., Murphy, D., and Thomson, D.: Observations of organic material in individual marine particles at Cape Grim during the First Aerosol Characterization Experiment (ACE 1), J. Geophys. Res., 103(D13), 16475–16483, doi:10.1029/97JD03719, 1998.
Mielonen, T., Arola, A., Komppula, M., Kukkonen, J., Koskinen, J., de Leeuw, G., and Lehtinen, K. E. J.: Comparison of CALIOP level 2 aerosol subtypes to aerosol types derived from AERONET inversion data, Geophys. Res. Lett., 36, L18804, doi:10.1029/2009GL039609, 2009.
Monahan, E. C., Spiel, D. E., and Davidson, K. L.: A model of marine aerosol generation via whitecaps and wave disruption, in: Oceanic whitecaps and their role in air-sea exchange processes, edited by: Monahan, E. and Niocaill, G. M., D. Reidel, Norwell, Mass, 167–174, 1986.
Moorthy, K. K. and Satheesh, S. K.: Characteristics of aerosols over a remote island, Minicoy in the Arabian Sea: optical properties and retrieved size characteristics, Q. J. Roy. Meteor. Soc., 126, 81–109, doi:10.1002/qj.49712656205, 2000.
Mulcahy, J. P., O'Dowd, C. D., Jennings, S. G., and Ceburnis, D.: Significant enhancement of aerosol optical depth in marine air under high wind conditions, Geophys. Res. Lett., 35, L16810, doi:10.1029/2008GL034303, 2008.
Murayama, T., Sugimoto, N., Uno, I., Kinoshita, K., Aoki, K., Hagiwara, N., Liu, Z., Matsui, I., Sakai, T., Shibata, T., Arao, K., Sohn, B., Won, J., Yoon, S., Li, T., Zhou, J., Hu, H., Abo, M., Iokibe, K., Koga, R., and Iwasaka, Y: Ground-based network observation of Asian dust events of April 1998 in East Asia, J. Geophys. Res., 106, 18345–18359, doi:10.1029/2000JD900554, 2001.
Murphy, D. M., Anderson, J. R., Quinn, P. K., McInnes, L. M., Brechtel, F. J., Kreidenweis, S. M., Middlebrook, A. M., P'osfai, M., Thomson, D. S., and Buseck, P. R.: Influence of sea-salt on aerosol radiative properties in the Southern Ocean marine boundary layer, Nature, 392, 62–65, doi:10.1038/32138, 1998.
ODowd, C. D., Facchini, M. C., Cavalli, F., Ceburnis, D., Mircea, M., Decesari, S., Fuzzi, S., Yoon, Y. J., and Putaud, J.-P.: Biogenically driven organic contribution to marine aerosol, Nature, 431, 676–680, doi:10.1038/nature02959, 2004.

ACPD
11, 4599–4630, 2011

O'Dowd, C. D. and de Leeuw, G.: Marine aerosol production: A review of the current knowledge, Phil. Trans. R. Soc. A: Mathematical, Phys. Eng. Sci., 365, 1753–1774, doi:10.1098/rsta.2007.2043, 2007.

O'Dowd, C., Scannell, C., Mulcahy, J., and Jennings, S. G.: Wind Speed Influences on Marine Aerosol Optical Depth, Adv. in Meteorol., 2010, 830846, doi:10.1155/2010/830846, 2010.

Omar, A. H. and Babakaeva, T.: Aerosol optical properties derived from lidar observations using cluster analysis, Geoscience and Remote Sensing Symposium, 2004, IGARSS '04, Proceedings, 2004 IEEE International, vol. 3, 2212–2215, doi:10.1109/IGARSS.2004.1370800, 2004.

Omar, A., Won, J., Winker, D., Yoon, S., Dubovik, O., and McCormick, M.: Development of global aerosol models using cluster analysis of Aerosol Robotic Network (AERONET) measurements, J. Geophys. Res., 110, D10S14, doi:10.1029/2004JD004874, 2005.

Omar, A., Winker, D., Vaughan, M., Hu, Y., Trepte, C., Ferrare, R., Lee, K., Hostetler, C., Kittaka, C., Rogers, R., Kuehn, R., Liu, Z.: The CALIPSO Automated Aerosol Classification and Lidar Ratio Selection Algorithm, J. Atmos. Ocean. Tech., 26, 1994–2014, doi:10.1175/2009JTECHA1231.1, 2009.

Pant, V., Deshpande, C. G., and Kamra, A. K.: On the aerosol number concentration–wind speed relationship during a severe cyclonic storm over south Indian Ocean, J. Geophys. Res., 113, D02206, doi:10.1029/2006JD008035, 2008.

Pierce, J. R. and Adams, P. J.: Global evaluation of CCN formation by direct emission of sea salt and growth of ultrafine sea salt, J. Geophys. Res., 111, D06203, doi:10.1029/2005JD006186, 2006.

Platnick, S. and Twomey, S.: Determining the susceptibility of cloud albedo to changes in droplet concentration with the advanced very high resolution radiometer, J. Appl. Meteor., 33(5), 334–347, 1994.

Prospero, J. M.: The chemical and physical properties of marine aerosols: An introduction, in: Chemistry of Marine Water and Sediments, edited by: Gianguzza, A., Pelizzetti, E., and Sammartano, S., Springer-Verlag, 35–82, 2002.

Rind, D., Chin, M., Feingold, G., Streets, D., Kahn, R. A., Schwartz, S. E., and Yu, H.: Modeling the Effects of Aerosols on Climate, in: Atmospheric Aerosol Properties and Climate Impacts, A Report by the US Climate Change Science Program and the Subcommittee on Global Change Research, edited by: Chin, M., Kahn, R. A., and Schwartz, S. E., National Aeronautics and Space Administration, Washington, DC, USA, 2009.

ACPD
11, 4599–4630, 2011

Rogers, R. R., Hair, J. W., Hostetler, C. A., Ferrare, R. A., Obland, M. D., Cook, A. L., Harper, D. B., Burton, S. P., Shinozuka, Y., McNaughton, C. S., Clarke, A. D., Redemann, J., Russell, P. B., Livingston, J. M., and Kleinman, L. I.: NASA LaRC airborne high spectral resolution lidar aerosol measurements during MILAGRO: observations and validation, Atmos. Chem. Phys., 9, 4811–4826, doi:10.5194/acp-9-4811-2009, 2009.

Sakai, T., Nagai, T., Zaizen, Y., and Mano, Y.: Backscattering linear depolarization ratio measurements of mineral, sea-salt, and ammonium sulfate particles simulated in a laboratory chamber, Appl. Optics, 49, 4441–4449, 2010.

Schulz, M., de Leeuw, G., and Balkanski, Y.: Sea-salt aerosol source functions and emissions, in: Emissions of Atmospheric Trace Compounds, edited by: Granier, C., Artaxo, P., Reeves, C., Springer, New York, USA, 333–359, 2004.

Sellegri, K., Villani, P., Picard, D., Dupuy, R., O'Dowd, C., and Laj, P.: Role of the volatile fraction of submicron marine aerosol on its hygroscopic properties, Atmos. Res., 90, 272–277, 2008.

Shaw, G. E.: Bio-controlled thermostasis involving the sulfur cycle, Climatic Change, 5(3), 297–303, doi:10.1007/BF02423524, 1983.

Smirnov, A., Holben, B., Eck, T., Dubovik, O., and Slutsker, I.: Effect of wind speed on columnar aerosol optical properties at Midway Island, J. Geophys. Res., 108(D24), 4802, doi:10.1029/2003JD003879, 2003a.

Smirnov, A., Holben, B., Dubovik, O., Frouin, R., Eck, T., and Slutsker, I.: Maritime component in aerosol optical models derived from Aerosol Robotic Network data, J. Geophys. Res., 108(D1), 4033, doi:10.1029/2002JD002701, 2003b.

Takemura, T., Nakajima, T., Dubovik, O., Holben, B. N., and Kinne, S.: Single-scattering albedo and radiative forcing of various aerosol species with a global three-dimensional model, J. Climate, 15, 333–352, 2002.

Vaughan, M. A., Young, S. A., Winker, D. M., Powell, K. A., Omar, A. H., Liu, Z., Hu, Y., and Hostetler, C. A.: Fully automated analysis of space-based lidar data: an overview of the CALIPSO retrieval algorithms and data products, Proc. SPIE, 5575, 16–30, 2004.

Vaughan, M. A., Winker, D. M., and Powell, K. A.: CALIOP Algorithm Theoretical Basis Document, Part 2: Feature Detection and Layer Properties Algorithms, PC-SCI-202, Release 1.01, 87 pp., NASA Langley Research Center, Hampton, VA, 56, available at: http://www-calipso.larc.nasa.gov/resources/pdfs/PC-SCI-202_Part2_rev1x01.pdf, 2005.

Vaughan, M. A., Powell, K. A., Winker, D. M., Hostetler, C. A., Kuehn, R. E., Hunt, W. H., Getzewich, B. J., Young, S. A., Liu, Z., and McGill, M. J.: Fully automated detection of cloud

ACPD
11, 4599–4630, 2011

and aerosol layers in the CALIPSO lidar measurements, J. Atmos. Ocean. Tech., 26, 2034–2050, 2009.
Wang, M. and Penner, J. E.: Aerosol indirect forcing in a global model with particle nucleation, Atmos. Chem. Phys., 9, 239–260, doi:10.5194/acp-9-239-2009, 2009.
Wang, C. S. and Street, R. L.: Transfers Across an Air-Water Interface at High Wind Speeds: The Effect of Spray, J. Geophys. Res., 83(C6), 2959–2969, doi:10.1029/JC083iC06p02959, 1978.
Weitkamp, C.: Lidar: range-resolved optical remote sensing of the atmosphere, Springer Science, 455 pp, 2005.
Welton, E. J., Voss, K. J., Quinn, P. K., Flatau, P. J., Markowicz, K., Campbell, J. R., Spinhirne, J. D., Gordon, H. R., and Johnson, J. E.: Measurements of aerosol vertical profiles and optical properties during INDOEX 1999 using micropulse lidars, J. Geophys. Res., 107(D19), 8019, doi:10.1029/2000JD000038, 2002.
Wentz, F. J. and Meissner, T.: AMSR Ocean Algorithm Theoretical Basis Document, Version 2, report number 121599A-1, Remote Sensing Systems, Santa Rosa, CA, 2000.
Wentz, F. J. and Meissner, T.: AMSR-E Ocean Algorithms, report number 051707, Remote Sensing Systems, Santa Rosa, CA, 6 pp., 2007.
Wentz, F. J., Gentemann, C., and Ashcroft, P.: On-orbit calibration of AMSR-E and the retrieval of ocean products, 83rd AMS Annual Meeting, American Meteorological Society, Long Beach, CA, 2003.
Winker, D. M. and Pelon, J.: The CALIPSO mission, Geoscience and Remote Sensing Symposium, IGARSS '03, Proceedings, IEEE International, 2, 1329–1331, 2003.
Winker, D. M., Vaughan, M. A., Omar, A. H., Hu, Y., Powell, K. A., Liu, Z., Hunt, W. H., and Young, S. A.: Overview of the CALIPSO Mission and CALIOP Data Processing Algorithms, J. Atmos. Ocean. Tech., 26, 2310–2323, 2009.
Young, S. A and Vaughan, M. A.: The retrieval of profiles of particulate extinction from Cloud Aerosol Lidar Infrared Pathfinder Satellite Observation (CALIPSO) data: Algorithm description, J. Atmos. Ocean. Tech., 26, 1105–1119, 2009.
Zhou, X. and Mopper, K.: Photochemical production of low molecular-weight carbonyl compounds in seawater and surface microlayer and their air-sea exchange, Mar. Chem., 56, 201–213, 1997.

ACPD
11, 4599–4630, 2011

Table 1. Regression statistics of aerosol optical depth vs. wind speed.

Regression relation	R^2	Reference
$AOD_{532} = \frac{-1.5}{11.9+1.102 \cdot e^{0.215 \cdot U_{10}}} + 0.1353$	0.97	Current work
$AOD_{500,SM} = 0.0068 \cdot U_{10} + 0.056$	0.14	Smirnov et al. (2003a)
$AOD_{550,cm} = 0.009 \cdot (U_{10} - 4) + 0.03$	0.50	Lehahn et al. (2010)
$AOD_{550,m} = 0.013 \cdot (U_{10} - 4) + 0.08$	0.45	Lehahn et al. (2010)
$AOD_{555,GL} = 0.00016 \cdot U_{10}^{2.3} + 0.036$	0.98	Glantz et al. (2009)
$AOD_{500,ML} = 0.00055 \cdot U^{2.195} + 0.06$	0.97	Mulcahy et al. (2008)
$AOD_{550,H} = 0.004 \cdot U_{10} + 0.085$	0.95	Huang et al. (2010)

ACPD
11, 4599–4630, 2011

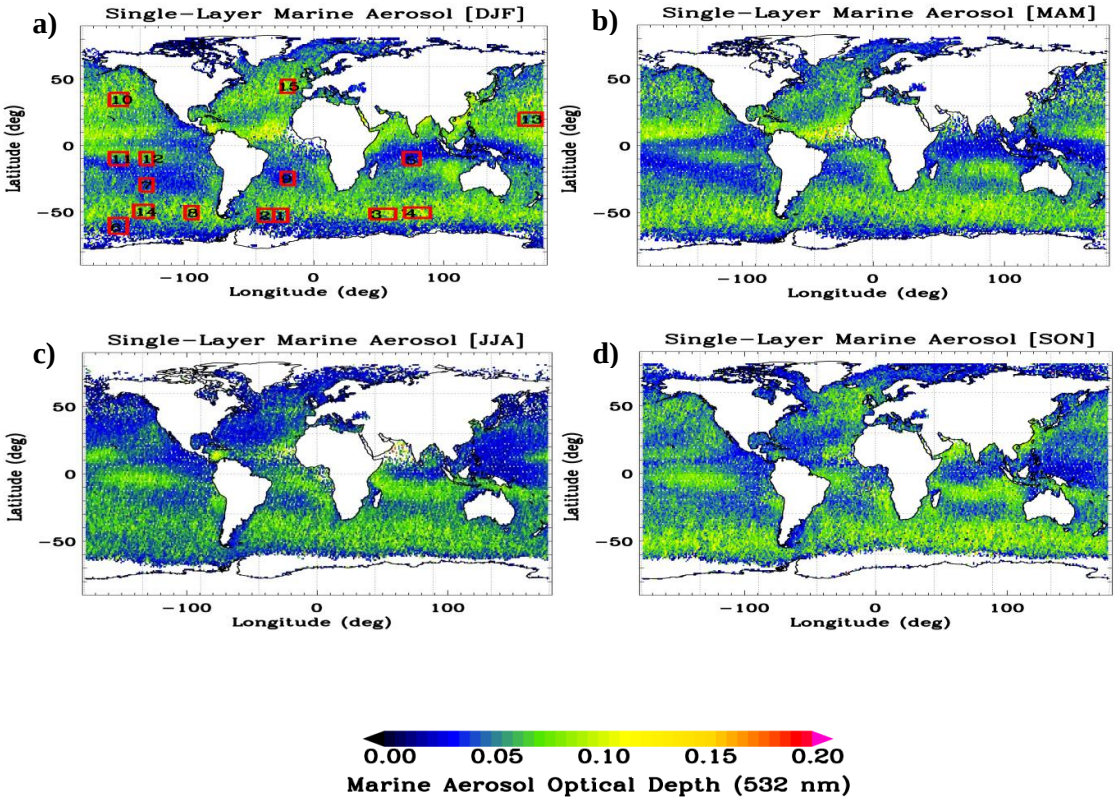

Fig. 1. Global distribution of 1° × 1° degree averaged CALIPSO level 2 version 3.01 mean AOD_{532} for "clean marine" single-layer aerosols. Layer optical depths are averaged for boreal winter (DJF), spring (MAM), summer (JJA), and fall (SON) from June 2006 to June 2010. Areas surrounded by solid red line in Fig. 1a illustrate the regions selected for the detailed analysis. Latitudes and longitudes of the selected 15 regions are summarized in Supplement Table S1.

ACPD
11, 4599–4630, 2011

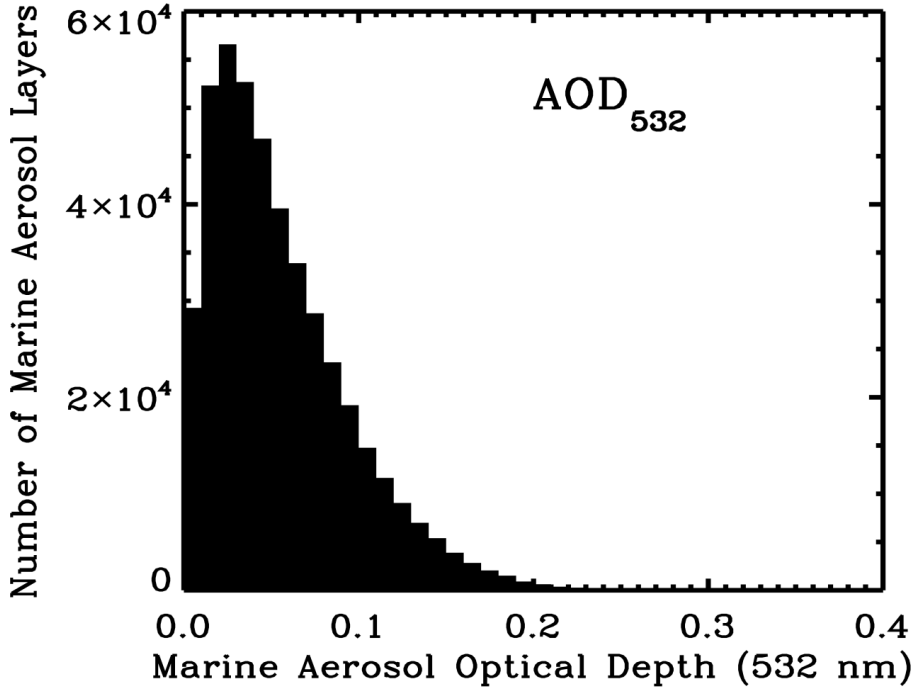

Fig. 2. The CALIPSO lidar maritime AOD_{532} histogram for 15 selected regions over the time period of June 2006 to June 2010.

ACPD
11, 4599–4630, 2011

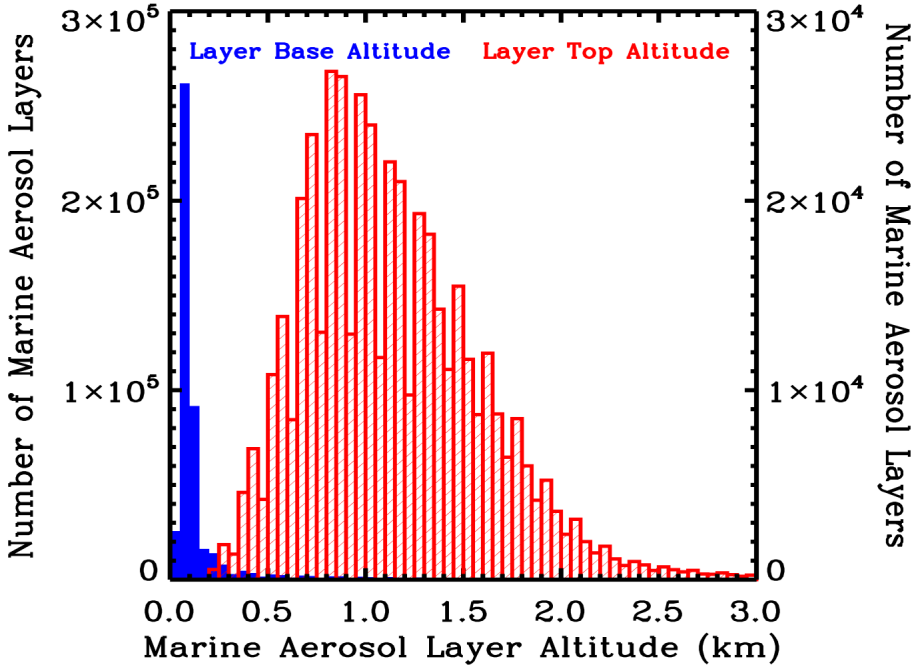

Fig. 3. The CALIPSO lidar histogram of maritime AOD_{532} aerosol layer base height (blue), and aerosol layer top height (red) for the 15 selected regions over the time period of June 2006 to June 2010.

ACPD
11, 4599–4630, 2011

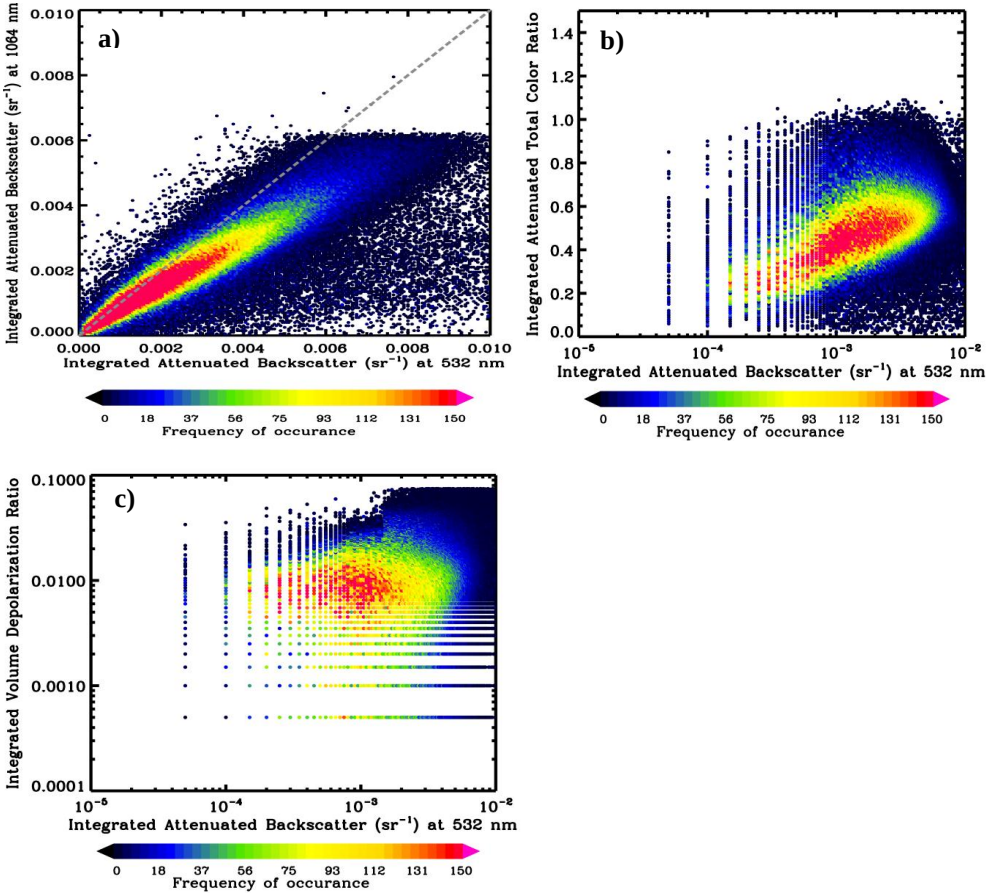

Fig. 4. The CALIPSO lidar relationships for **(a)** β_{1064}–β_{532} **(b)** $\chi - \beta_{532}$ and **(c)** δ_v–β_{532} for 15 selected regions over the time period of June 2006 to June 2010. The color of each pixel represents the frequency of occurrence and the dashed line on Fig. 4a indicates 1:1 ratio.

ACPD
11, 4599–4630, 2011

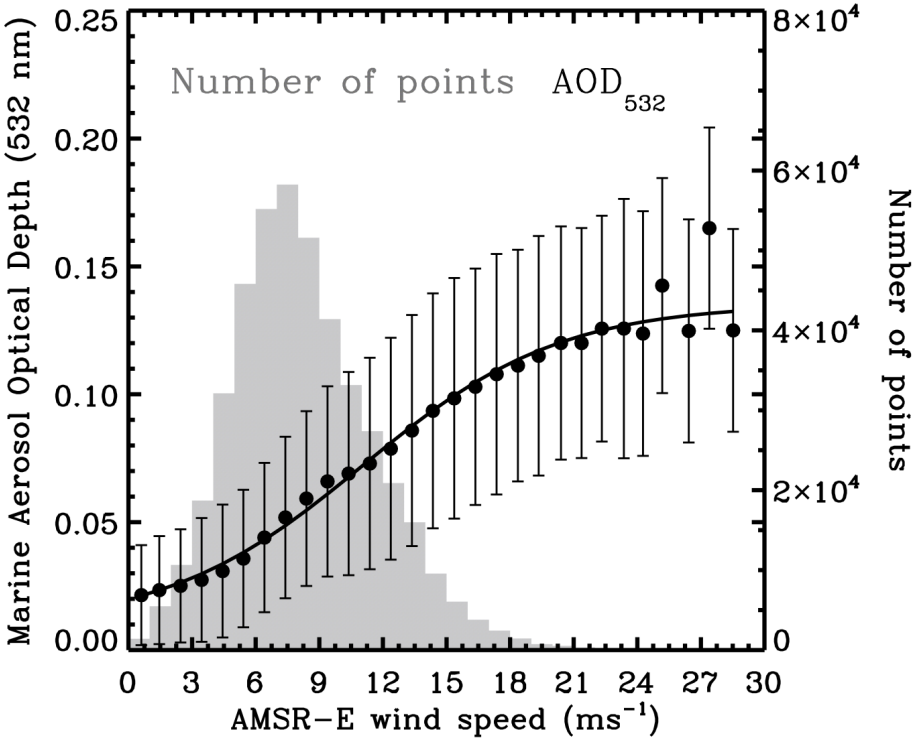

Fig. 5. The relationship between CALIPSO AOD_{532} and AMSR-E wind speed for 15 selected regions over the time period of June 2006 to June 2010. The analysis is based on a total 443 231 collocated data points of AOD and wind speed. The number of available data points for each wind speed bin is plotted at the background in grey color. Circles and error bars show mean values and standard deviation of AOD for each 1 m s^{-1} wind speed bin, respectively. Logistic regression relationship between AOD_{532} and wind speed is shown with the solid black line.

ACPD
11, 4599–4630, 2011

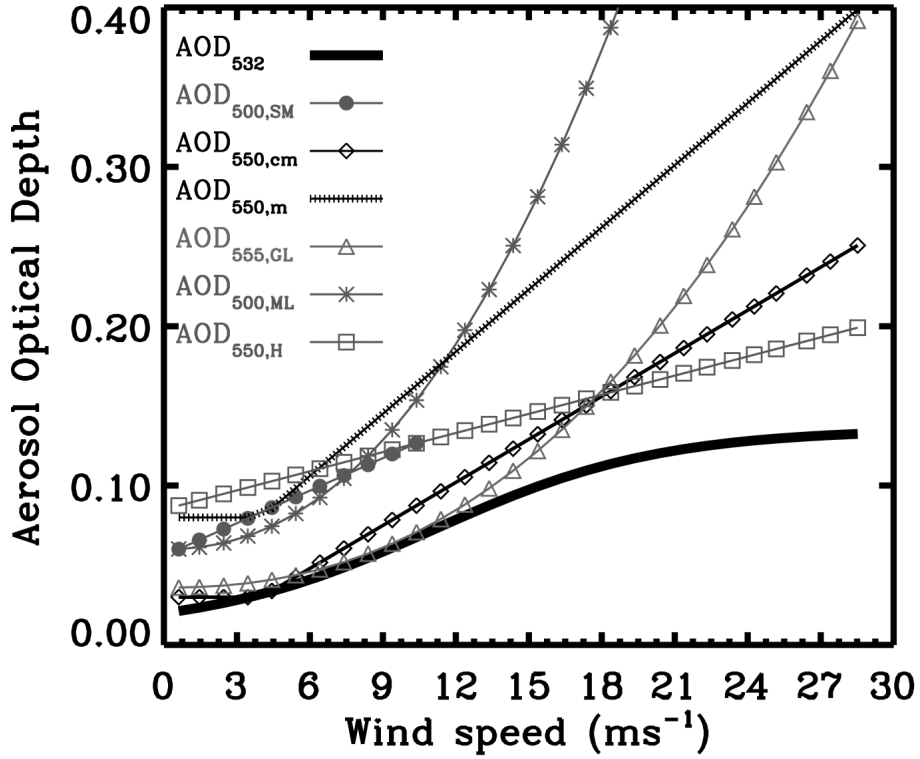

Fig. 6. Maritime aerosol optical depth as a function of wind speed. The regression statistics and the acronyms are summarized in Table 1. See text for more details.

ACPD
11, 4599–4630, 2011